Yerbilimleri, 2025, 46 (3), 176-201, 1751771

Hacettepe Üniversitesi Yerbilimleri Uygulama ve Araştırma Merkezi Bülteni (*Bulletin of the Earth Sciences Application and Research Centre of Hacettepe University)*

YERBİLİMLERİ
Bulletin for Earth Sciences

ISSN: 2687- 2978

Opal Mineralizasyonu ve Oluşum Koşulları: Seydiler Havzası'ndaki (Afyonkarahisar, Batı Türkiye) Diyatomitlerin Silisleşme Süreçleri

Opal Mineralization and Formation Conditions: Silicification Processes of Diatomites from Seydiler Basin (Afyonkarahisar, Western Türkiye)

EVRİM ÇOBAN [1*], GÜRSEL YANIK [2], MURAT HATİPOĞLU [3] , AHMET YILDIZ [4]

[1] Muğla Sıtkı Koçman Üniversitesi, Milas Meslek Yüksekokulu, Muğla, Türkiye

[2] Kütahya Dumlupınar Üniversitesi, Jeoloji Mühendisliği Bölümü, Kütahya, Türkiye

[3] Dokuz Eylül Üniversitesi, İzmir Meslek Yüksekokulu, El Sanatları Bölümü, İzmir, Türkiye

[4] Afyon Kocatepe Üniversitesi, Jeoloji Mühendisliği Bölümü, Afyon, Türkiye

Received *(geliş)*: 26 July (*Temmuz*) 2025 Accepted *(kabul):* 7 December (*Aralık*) 2025

ABSTRACT

The Seydiler opal deposit (Afyonkarahisar, Türkiye) represents a rare example of gem-quality opal formed in a lacustrine, non-hydrothermal environment. This study characterizes these opals using mineralogical, geochemical, isotopic and gemological methods, revealing that biogenic siliceous ooze derived from diatomaceous accumulation served as the primary precursor during low-temperature burial diagenesis. Mineralogical analyses (XRD, FTIR, Raman) show that the opals are mainly composed of pseudo-crystalline silica phases dominated by opal-CT, with minor opal-C and trace α-quartz. Oxygen isotope values ($\delta^{18}O$ = 23.86–25.29‰ V-SMOW) indicate formation temperatures of ~32–51 °C, consistent with the opal-A to opal-CT transition under suboxic, meteoric-fluid conditions. Geochemical data reveal high SiO_2 contents (>93 wt.%) and enrichments in Zn, Cs, Rb, Sr and U, reflecting combined biological uptake, early diagenetic remobilization and distal Neogene pyroclastic input. SEM analyses document exceptionally preserved diatom assemblages, including first-reported taxa such as Staurosira construens and two morphotypes of Staurosirella pinnata, indicating minimal post-depositional disturbance. Gemological examination confirms vivid natural color zoning, vitreous–waxy luster, RI ≈ 1.451 and SG 2.18–2.30, supporting their classification as gem-quality opals. Hydration-sensitive samples show potential for dehydration cracking, highlighting the need for stabilization.

Keywords: Biogenic Opal, Diatomite, Lacustrine Silica, Opal, Seydiler Opal

ÖZ

Seydiler opal yatağı (Afyonkarahisar, Türkiye), hidrotermal olmayan gölsel bir ortamda oluşmuş değerli taş kalitesindeki opallerin nadir örneklerinden biridir. Bu çalışma, opallerin mineralojik, jeokimyasal, izotopik ve gemolojik özelliklerini belirlemiş; diyatom kaynaklı biyojenik silisli çamurun düşük sıcaklıklı gömülme diyajenezi

sırasında opal oluşumunun ana öncül malzemesi olduğunu göstermiştir. Mineralojik analizler (XRD, FTIR, Raman), opallerin başlıca opal-CT'den oluştuğunu, az miktarda opal-C ve iz α-kuvars içerdiğini ortaya koymuştur. Oksijen izotop değerleri ($\delta^{18}O$ = 23.86–25.29‰ V-SMOW), yaklaşık 32–51 °C oluşum sıcaklıklarına işaret ederek opal-A → opal-CT dönüşümüne karşılık gelmektedir. Jeokimyasal veriler, yüksek SiO_2 içerikleri (> %93) ile Zn, Cs, Rb, Sr ve U zenginleşmelerini göstermekte olup biyolojik element alımı, diyajenezik mobilizasyon ve uzak Neojen piroklastik girdilerin ortak etkilerini yansıtmaktadır. SEM görüntüleri, Staurosira construens ve Staurosirella pinnata'nın iki yeni morfotipi dâhil olmak üzere olağanüstü korunmuş diyatom topluluklarını ortaya koymuştur. Gemolojik incelemeler, belirgin renk zonlanmaları, cam–yağsı parlaklık, ~1.451 kırılma indisi ve 2.18–2.30 özgül ağırlık değerleri ile örneklerin değerli taş niteliğini doğrulamaktadır. Su kaybına bağlı çatlama riski taşıyan örneklerde stabilizasyon önerilmektedir.

Anahtar Kelimeler: *Biyojenik Opal, Diyatomit, Gölsel Silis, Opal, Seydiler Opali*

https://doi.org/10.17824/yerbilimleri.1751771

* Corresponding Author/Sorumlu Yazar: evrimcoban@mu.edu.tr

INTRODUCTION

An ooze is a biogenic sediment that accumulates in marine or non-marine basins through the deposition of microscopic skeletal remains of planktonic and benthic organisms. Following their death, siliceous microorganisms (e.g., diatoms, radiolarians) or calcareous microorganisms (e.g., foraminifera, coccolithophores) settle on the basin floor, forming siliceous or calcareous ooze. These biogenic sediments typically consist of at least 30% microfossil content and may lithify through diagenetic processes to become rocks such as diatomite (from siliceous ooze) or chalk (from calcareous ooze) (Easton et al., 1982; Hoek et al., 1995; Del Amo et al., 1997; Coradin & Lopez, 2003; Fuhrmann & Landwehr, 2004; Sims et al., 2006; Lange-Bertalot et al., 2017).

Siliceous oozes primarily consist of hydrated amorphous silica (opal-A), which originates from diatom frustules, radiolarians, and other siliceous plankton. Diatoms are taxonomically divided into centric forms (radially symmetrical, pelagic) and pennate forms (bilaterally symmetrical, benthic), each with unique ecological distributions (Kröger, 2007; Medlin, 2009). Although the functional morphology and pore morphometry of centric and pennate diatoms appear broadly similar, the structure of diatom frustules may affect light-harvesting and biomineralization efficiency (Finkel & Benjamin, 2010; Herve et al., 2012).

While numerous diatomite deposits have been documented across Türkiye (Bircan, 1968; Uygun, 1976; Işık, 1984; Açıkalın, 1991; Gürel & Yıldız, 2007), none have previously been identified as hosts of gem-quality opal deposits. The Seydiler Basin (Afyonkarahisar) represents the first recorded occurrence of such a system, where multicolored opals are hosted within a lacustrine, diatomite-dominated stratigraphy. Although the diatomite potential of the region was first evaluated by Ergün (1969) in the Hasan Abdullah Gediği area, and later by Işık (1984), Yıldız (1997), and Yıldız et al. (2003), no prior study has investigated the mineralogical, geochemical, and gemological significance of the opaline material or interpreted the deposit as a non-marine ooze hosting economic opal.

In this context, the sedimentary sequence of the Seydiler Basin is newly defined as the Seydiler Ooze, a Miocene-aged lacustrine succession composed of interbedded diatomite and tuffite, overlying a basaltic–andesitic volcanic cover and underlain by a metamorphic basement (Andolfato, 1969; Bargu, 1991; Aydar et al., 1998; Özkaymak et al., 2017). The

area is also known for its unique surficial geomorphology and historical significance within the Phrygian Valley (Figure 1). Gem opals were first discovered serendipitously during mining operations near the Karakaya village, with continuous opaline layers reaching up to 80 cm thick along the slopes of Topyeri, Karakaya, Yatakyeri, and Kel Tepe (Çoban, 2020).

The present study aims to provide the first comprehensive characterization of the Seydiler gem-quality opals in terms of mineralogy, geochemistry, isotopes, and gemology. The research is structured around three core objectives:

1. To determine the mineralogical and chemical composition of the opals using XRF, ICP-MS, XRD, FTIR, and Raman spectroscopy,
2. To estimate formation temperatures based on $\delta^{18}O$ isotope data and silica–water fractionation models,
3. To assess the gemological properties of selected samples, including refractive index, specific gravity, UV fluorescence, and post-mining durability related to molecular water content. This investigation provides unique insight into the genesis and preservation of lacustrine-hosted, gem-quality opals in Türkiye. It offers a globally rare example of biogenic silica transformation within a non-marine ooze setting.

GEOLOGICAL SETTING

The Afyon Zone is one of the major tectonic domains in western Türkiye, composed of a Paleozoic metamorphic basement and a Mesozoic cover sequence, followed by extensive Cenozoic volcanic and sedimentary successions (Okay, 1984; Candan et al., 2005; Özdamar et al., 2013). The basement includes prominent units such as the Doğanlar schist and İscehisar marble, representing low- to medium-grade metamorphic rocks.

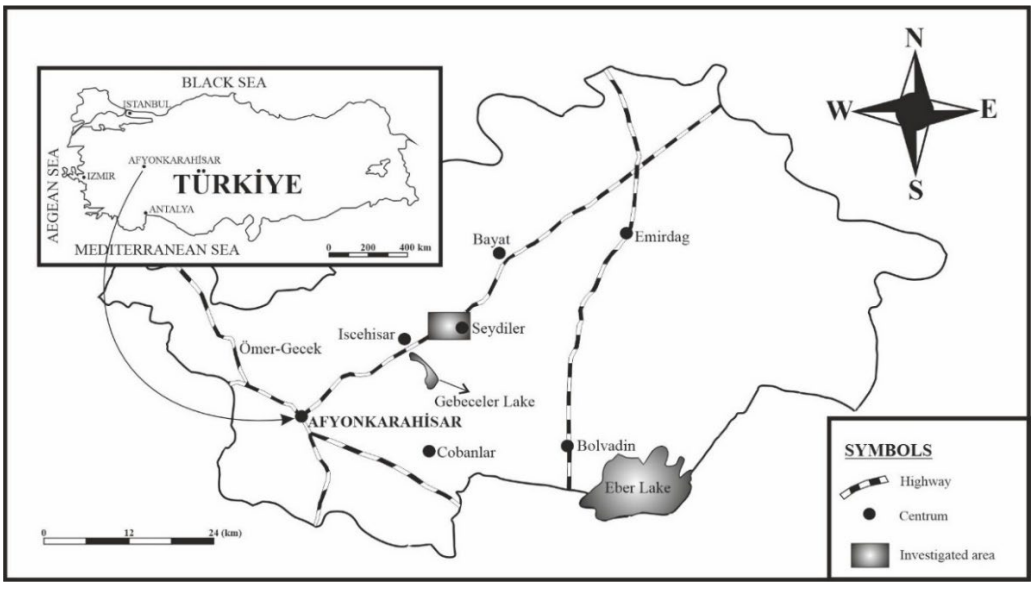

Figure 1. The location map of study area.

Şekil 1. *Çalışma alanının yer bulduru haritası.*

The Seydiler area, which hosts the studied opal deposit, lies within the Cenozoic volcanic belt of the Afyon Zone. Here, the metamorphic basement is unconformably overlain by thick ignimbrite layers and lava flows, forming the base of the Seydiler volcanic stratigraphy (Andolfato, 1969; Metin et al., 1987; Bargu, 1991; Yıldız, 1997; Aydar et al., 1998; Prelević et al., 2012; Akal et al., 2013; Özkaymak et al., 2017). Archaeological evidence suggests proximity to ancient Phrygian settlements, further enhancing the region's geo-cultural significance (Özkaymak et al., 2017). The Seydiler volcanic sequence consists of thick-bedded, cream-to-grayish pyroclastic rocks, primarily tuffs and agglomerates (Kuşcu & Yıldız, 2001). Intercalated within these are tabular diatomite beds, which are prominently exposed near Seydiler village. These biogenic siliceous horizons are overlain by dark-colored, trachyandesitic lava flows displaying characteristic flow banding and tabular, subhorizontal morphologies (Kuşcu et al., 2006).

In the upper portions of the sequence, alternating tuff and diatomite layers form rhythmic successions. Diatomite outcrops extend across an area of ~1.5 km² between the Keltepe and Karakaya localities, where the diatomite tuff stratigraphy attains a cumulative thickness of up to 26 m (Yıldız et al., 1999). The diatomite is predominantly white to pale gray, with occasional yellowish to cream tones caused by iron oxide staining or detrital admixtures. Bedding planes are nearly horizontal around Karakaya (Figure 2). A particularly significant feature is the occurrence of a stratiform opal horizon, ranging in thickness from 0.3 to 1.0 m, developed at the uppermost contact of the diatomite sequence. The overlying pyroclastic units conformably overlie this layer and represent the principal source of common and gem-quality opal in the Seydiler deposit (Figure 3).

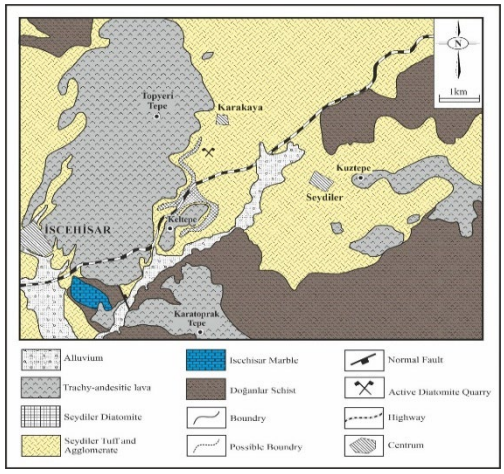

Figure 2. The geological map of the Seydiler area, showing the distribution of diatomite, tuffs, and trachyandesitic lavas (Modified from Metin et al., 1987; Yıldız, 1997).

***Şekil 2**. Seydiler yöresinin diatomit, tüf ve trakiandezit lavların dağılımını gösteren jeoloji haritası (Metin ve diğ., 1987; Yıldız, 1997'den değiştirilmiştir).*



Figure 3 (a): Satellite image (Google Earth™) showing the Seydiler quarry area. (b): Field view of the active quarry's exposed stratigraphy shows diatomite level, tuffs, and overlying trachyandesitic flows.

***Şekil 3.** (a): Seydiler taş ocağı alanını gösteren uydu görüntüsü (Google Earth™). (b): Aktif taş ocağının açığa çıkmış stratigrafisinin saha görünümü, diyatomit seviyelerini, ara tabakalı tüfleri ve üstteki trakiandezit akışlarını göstermektedir.*

MATERIALS AND METHODS

A comprehensive geological survey was conducted over an area of approximately 50 km² in the Seydiler Basin (Afyonkarahisar, Turkey), focusing on the Miocene-aged lacustrine volcano-sedimentary succession informally known as the Seydiler Ooze. This sequence comprises interbedded diatomite, tuff, and stratiform opal-bearing horizons. The thickest and most laterally continuous opaline units are primarily exposed in vertical sections near the Karakaya locality, where individual opal layers can reach thicknesses of up to 80 cm. These layers can be traced laterally for several meters within the diatomite-tuff alternations.

During the field studies, numerous opal occurrences were documented across various outcrops, displaying multiple colours, including reddish-brown, green, yellowish-green, champagne, and blackish-grey. However, not all color variants were equally suitable for mineralogical or spectroscopic analysis. Some specimens, particularly those with champagne and blackish-grey hues, showed signs of significant surface weathering, microfracturing due to dehydration, and pigment leaching, likely resulting from prolonged atmospheric exposure or late-stage fluid interactions. Such post-depositional changes may obscure essential textural and spectral features crucial for accurate interpretation.

Two samples, S2-8 (reddish-brown to green) and S2-9 (yellowish-green), were chosen for detailed geochemical and mineralogical characterization (Figure 4). The selection was based on the following criteria:

Stratigraphic integrity: Both specimens were collected from laterally persistent and well-defined stratigraphic levels, avoiding isolated lenses or zones prone to alteration that could compromise their representativeness.

Textural and mineralogical preservation: The opals selected exhibit dense colloform textures with few signs of weathering. SEM imaging validates preserving key biogenic features, including partially intact diatom frustules and siliceous imprints.

Color abundance and geochemical significance: Reddish and greenish hues are the most common in the field and are believed to reflect variations in Fe, Mn, and U content, necessitating targeted trace element analyses.

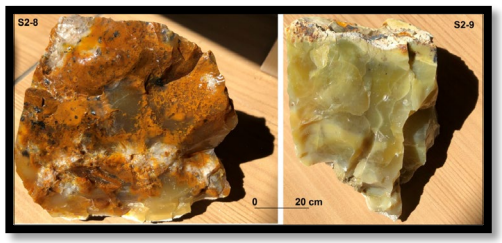

Figure 4. Representative opals from the Seydiler deposit: reddish-brown (S2-8) and yellowish-green (S2-9) specimens. Both samples show a vitreous to waxy luster and contain blackish speckles. These two-color varieties are the most abundant and economically significant types observed in the field. They were selected for detailed physicochemical and spectroscopic analyses. The scale bar represents 20 cm (Çoban, 2020).

Şekil 4. *Seydiler yatağından temsili opaller: kırmızımsı kahverengi (S2-8) ve sarımsı yeşil (S2-9) örnekler. Her iki örnek de camsı ila mumsu parlaklıkta olup siyahımsı benekler içermektedir. Bu iki renkli çeşitler, sahada gözlemlenen en bol ve ekonomik açıdan en önemli türlerdir. Ayrıntılı fizikokimyasal ve spektroskopik analizler için seçilmişlerdir. Ölçek çubuğu 20 cm'yi temsil etmektedir (Çoban, 2020).*

Analytical methods

X-ray diffraction (XRD)

The mineralogical composition of opal samples was determined by powder XRD using a Malvern-Panalytical Empyrean diffractometer

equipped with a Cu anode ($K\alpha_1$ = 1.54060 Å, $K\alpha_2$ = 1.54443 Å). Operational settings included 45 kV and 45 mA, with a 2θ scanning range of 5° to 70°, a step size of 0.013°, and a count time of 58.395 s per step. Crystalline phases were identified through comparison with the ICSD and COD databases using HighScore Plus software (version 4.9). XRD measurements were carried out at the ILTEM, University of Kütahya Dumlupınar University.

Major, trace and rare earth element Geochemistry

Major element compositions of opals were determined by XRF, while trace elements were quantified via inductively coupled plasma mass spectrometry (ICP-MS). Volatile content was assessed using the Loss on Ignition (LOI) method. These analyses were conducted at ACME Analytical Laboratories in Canada. XRF and LOI were also used to analyze diatomite samples (codes UL, ML, and LL) at the ILTEM Laboratory, Kütahya Dumlupınar University.

Fourier-transform infrared spectroscopy (FT-IR)

FT-IR spectra were obtained from opal and diatomite samples using a Bruker FT-IR system with a CsI beam splitter and a DTGS detector. Spectra were recorded in the 400–4000 cm^{-1} range at 2 cm^{-1} resolution. Post-acquisition processing included baseline correction, smoothing, and normalization. All FT-IR work was conducted at the ILTEM Laboratory, Kütahya Dumlupınar University.

Raman spectroscopy

The opals' Raman spectra were collected using a HORIBA Jobin Yvon XPLORA micro-Raman system coupled to an Olympus BM-41 microscope. A 532 nm He–Ne laser was employed as the excitation source. The system provided 1 cm^{-1} spectral resolution over the 50–4000 cm^{-1} range. Spectra were measured under ambient lighting on dark backgrounds. Analyses were performed at the Gemological Testing Laboratory, Dokuz Eylül University.

Scanning electron microscopy & EDX (SEM-EDS) and cathodoluminescence (CL)

Surface morphology and microtextures of opal and diatomite samples were observed using an FEI Nova NanoSEM 650 instrument. Samples were Au–Pd coated using a Denton Vacuum Desk V sputter-coater. SEM-EDS investigations were conducted at the ILTEM Laboratory, Kütahya Dumlupınar University. Cathodoluminescence analyses were performed on the Gatan MonoCL4 device.

Stable oxygen isotopes ($\delta^{18}O$):

Stable $\delta^{18}O$ isotope ratios were measured on samples S2-8 and S2-9 using a Thermo Finnigan TC/EA IRMS system operated under the V-SMOW calibration scale. Each opal aliquot (~600 µg) was loaded into silver capsules and combusted in a 1450 °C elemental analyzer. Helium was used as a carrier gas. Isotope measurements were performed at TÜBİTAK-MAM Laboratory (Türkiye).

Gemological tests

Gemological testing was conducted at the DGL Gemological Testing Laboratory, Dokuz Eylül University. Specific gravity was measured hydrostatically using an electronic balance with a precision of 0.001 g. Refractive index, optical character, and optic sign were determined using an Eickhorst SR/XS refractometer with a contact liquid (RI=1.79) under a 589 nm quartz lamp. Ultraviolet (UV) luminescence responses were evaluated using both long-wave (366 nm) and short-wave (255 nm) excitation sources.

RESULTS

Mineralogy, morphology, and structural characterization

X-ray diffraction (XRD) studies

X-ray diffraction (XRD) patterns of representative Seydiler opals (S2-8 and S2-9) display broad yet distinct peaks centered at d = 4.11 Å and d = 2.51 Å, characteristic of opal-CT (disordered cristobalite–tridymite intergrowth) and incipient opal-C, respectively. These features indicate a transitional silica assemblage evolved from biogenic opal-A through low-temperature burial diagenesis (Figure 5). Sample S2-9 shows sharper and more intense peaks, suggesting a higher degree of structural ordering compared to S2-8, whose broader peaks reflect residual opal-A characteristics. A secondary reflection at d = 4.32 Å, more prominent in S2-8, is also linked to opal-CT and may represent local tridymite-type stacking domains. In addition to the main opaline phases, weak reflections at d = 2.05 Å, 1.64 Å, and 1.44 Å are attributed to microcrystalline α-quartz. The presence of α-quartz is best interpreted as a detrital inclusion mineral, most likely introduced during sedimentation, possibly from volcanic ash or reworked siliceous material.

A peak at d = 3.03 Å observed in S2-8 corresponds to the (104) reflection of calcite, while a minor peak at d = 2.28 Å may also be linked to carbonate phases. The occurrence of calcite can be attributed to two complementary processes:

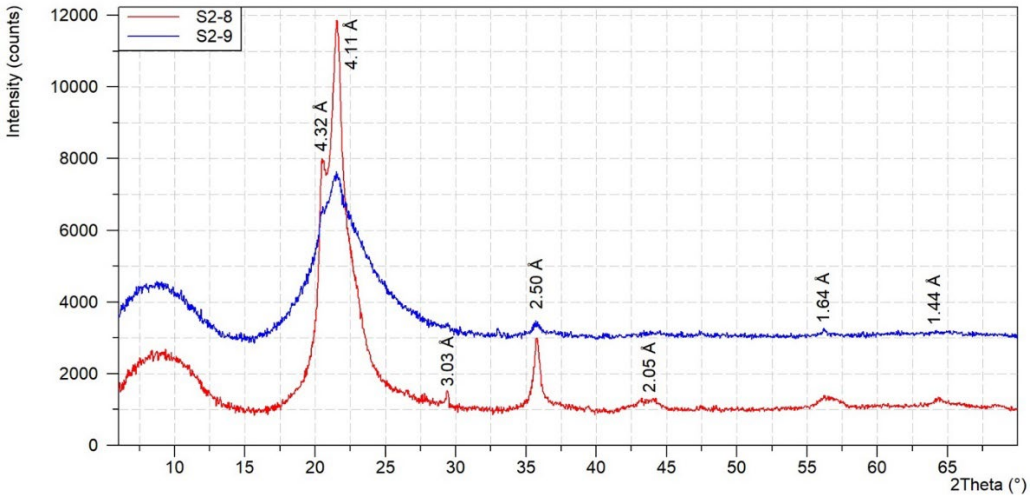

Figure 5. XRD patterns of S2-8 and S2-9 show dominant peaks at d = 4.11 Å and 2.51 Å, indicating opal-CT and transitional opal-C. A reflection at 4.32 Å supports opal-CT, while a 3.03 Å peak in S2-8 suggests calcite. Additional weak peaks reflect the presence of trace α-quartz and ongoing diagenetic transformation from opal-A.

***Şekil 5**. S2-8 ve S2-9'un XRD desenleri, d = 4,11Å ve 2,51Å'de baskın tepe noktaları göstermektedir ve bu da opal-CT ve geçiş opal-C'yi göstermektedir. 4,32Å'deki bir yansıma opal-CT'yi desteklerken, S2-8'deki 3,03Å'lik bir tepe noktası kalsit olduğunu göstermektedir. Ek zayıf tepe noktaları, eser miktarda α-kuvars varlığını ve opal-A'dan devam eden diyajenetik dönüşümü yansıtmaktadır.*

- Authigenic precipitation from Ca-rich, slightly alkaline lacustrine pore waters during early diagenesis.
- Volcaniclastic alteration, such as plagioclase breakdown, which releases Ca^{2+} into the system and promotes carbonate formation.

The spatial association of calcite with opaline zones suggests simultaneous, co-diagenetic precipitation from evolving fluids during shallow burial. The overall mineral assemblage, comprising opal-CT, minor opal-C, sporadic α-quartz, and calcite, supports a non-hydrothermal, lacustrine diagenetic model characterized by variable fluid–rock interactions under low-temperature conditions.

Scanning electron microscope (SEM) studies

High-resolution SEM analyses were conducted to investigate the microstructural and mineralogical features of the Seydiler opals, with a special focus on dendritic structures and associated evaporitic minerals. Densely branched, frond-like dendritic patterns (~2–15 µm) were observed across the opal specimens, consistent with manganese oxide precipitation. Their radial symmetry, fine branching, and localization along pore walls and fractures suggest formation of Mn-oxide phases (e.g., pyrolusite, birnessite) under suboxic–oxic conditions. Embedded in a compact silica matrix, these dendrites often nucleate along pore edges, indicating late-stage diagenetic growth driven by redox fluctuations (Figure 6).

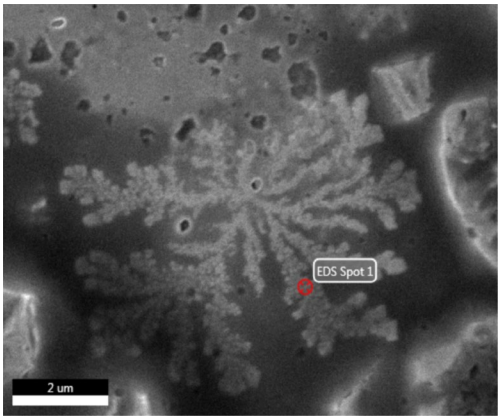

Figure 6. SEM image showing a well-developed, radially branched dendritic Mn-rich structure embedded in a compact opaline matrix. EDS Spot 1 is marked on the dendrite.

Şekil 6. *Kompakt opalin bir matrise gömülü, iyi gelişmiş, radyal olarak dallanmış dendritik Mn açısından zengin bir yapıyı gösteren SEM görüntüsü. EDS Spot 1 dendrit üzerinde işaretlenmiştir.*

Spot analyses performed on the dendritic regions consistently returned elevated manganese contents (up to 8.10 wt.%), confirming their identity as Mn-rich phases. Accompanying elemental peaks for Na, Cl, and K were also detected in varying concentrations, particularly in areas directly surrounding the dendrites. This co-localization implies the presence of evaporitic mineral phases, most likely halite (NaCl), sylvite (KCl), and possibly $MnCl_2$. Representative EDS spectra (Figure 7) confirm this interpretation.

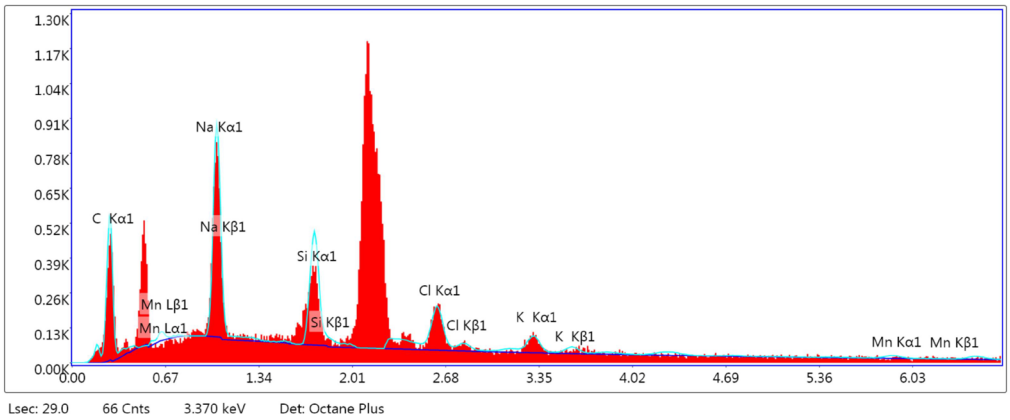

Figure 7. EDS spectrum corresponding to Spot 1 on the dendritic Mn-rich structure.

Şekil 7. *Dendritik Mn açısından zengin yapıdaki Nokta 1'e karşılık gelen EDS spektrumu.*

In addition to dendrites, SEM images revealed polygonal to subangular particles intergrown with opaline silica, likely representing siliceous fragments or halite microcrystals along microfractures. EDS maps show spatial overlap of Mn, Na, Cl, and C, supporting co-precipitation under evaporitic diagenetic conditions. These features Mn oxides, salt residues, and biogenic carbon collectively suggest opal formation in a shallow lacustrine setting influenced by redox stratification, episodic evaporation, and active biogeochemical processes.

The scanning electron microscopy (SEM) was employed to investigate the diatomaceous sequence in the Seydiler Basin. This analysis offers insights into the stratigraphic evolution, depositional dynamics, and biogenic silica accumulation, all of which are essential to the formation of stratiform opal layers. SEM images from these stratigraphic sequences reveal diverse and well-preserved diatom frustules (Figure 8; 9), substantiating a biogenic source for the amorphous silica. Taxa include Ellerbeckia sp., Eunotia sp., Gomphonema sp., Halamphora sp., and Pinnularia sp., which indicate nutrient-rich, freshwater lacustrine environments. The frustules retain intricate features such as costae and raphes, implying stable, low-energy depositional conditions conducive to excellent fossil preservation.

Finer centric and araphid pennate forms were also identified, particularly Staurosira construens (Ehrenberg, 1843) and Staurosirella pinnata (Ehrenberg, 1843). Their morphology, including high surface area and fine perforations, likely facilitated efficient silica accumulation. These taxa contributed opal-A precursor material to the diatomite matrix, supporting a low-temperature silicification process.

This study confirms previously identified diatom genera in the Seydiler ooze and documents three new species: Staurosira construens (Ehrenberg, 1843), Straurosirella pinnata (Ehrenberg, 1843) 3, and Straurosirella pinnata (Ehrenberg, 1843) 6. Geochemical and morphological data point to a lacustrine paleoenvironment rich in biogenic silica. The upper diatomite unit is the most favourable horizon for gem-quality opal development due to its high SiO_2 content, low detrital input, and optimal biological productivity. These findings collectively support a model of low-temperature diagenetic transformation of biogenic silica into

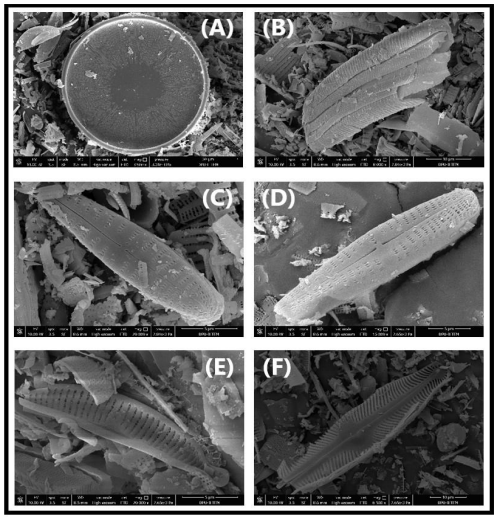

Figure 8. Scanning electron micrographs of freshwater diatom taxa identified within the Seydiler lacustrine diatomite represent high biogenic silica productivity. (A) Ellerbeckia sp. (centric diatom) with well-preserved radial symmetry and robust frustule structure; (B) Eunotia sp., a benthic araphid pennate species characterized by curved, bilaterally symmetrical valves; (C–D) Gomphonema sp. showing asymmetrical, clavate frustules with a prominent central area and striae patterning; (E) Halamphora sp. displaying dorsiventral valve outline and coarse striae; (F) Pinnularia sp., an elongated pennate form with clear axial and central areas and strongly developed costae (from Çoban, 2020).

Şekil 8. *Seydiler göl diyatomitinde tanımlanan tatlı su diyatome taksonlarının taramalı elektron mikroskobu görüntüleri yüksek biyojenik silika verimliliğini göstermektedir. (A) İyi korunmuş radyal simetri ve güçlü früstül yapısına sahip Ellerbeckia sp. (merkezli diyatom); (B) Kavisli, bilateral simetrik kapakçıklarla karakterize bentik bir araphid pennat türü olan Eunotia sp.; (C–D) Belirgin bir merkezi alan ve çizgili desene sahip asimetrik, klavat früstüller gösteren Gomphonema sp.; (E) Dorsiventral kapakçık ana hatları ve kaba çizgiler gösteren Halamphora sp.; (F) Net eksenel ve merkezi alanlara ve güçlü gelişmiş kostalara sahip uzunlamasına pennat formu olan Pinnularia sp. (Çoban, 2020'den).*

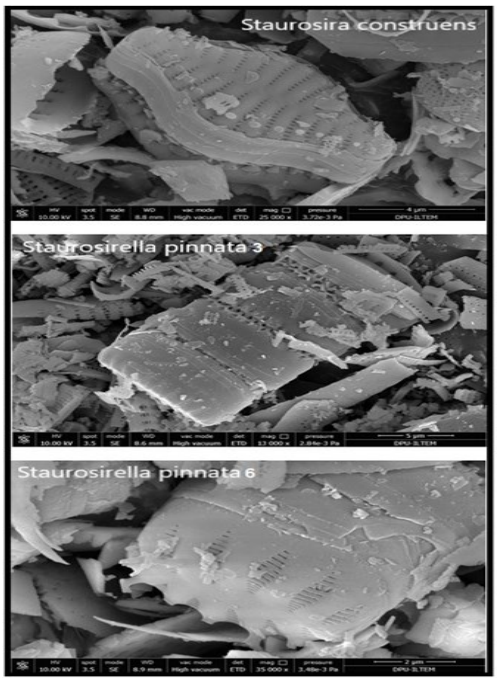

Figure 9. Scanning electron micrographs of freshwater diatoms identified in the Seydiler lacustrine diatomite. (A) Staurosira construens (Ehrenberg, 1843) showing araphid pennate structure with finely patterned striae and robust frustule morphology. (B–C) Staurosirella pinnata (Ehrenberg, 1843) exhibits densely ornamented valves with a clear separation between costae and striae, indicative of eutrophic lacustrine conditions. These araphid pennate diatoms are among the dominant taxa contributing to biogenic silica accumulation in the Seydiler ooze sequence (from Çoban, 2020).

Şekil 9. *Seydiler göl diyatomitinde tanımlanan tatlı su diyatomlarının taramalı elektron mikroskobu görüntüleri. (A) İnce desenli çizgiler ve güçlü früstül morfolojisine sahip araphid pennat yapısı gösteren Staurosira construens. (B–C) Staurosirella pinnata, ötrofik göl koşullarının göstergesi olan, kosta ve çizgiler arasında belirgin bir ayrım bulunan, yoğun süslü kapakçıklar sergiliyor. Bu araphid pennat diyatomları, Seydiler ooze dizisindeki biyojenik silika birikimine katkıda bulunan baskın taksonlar arasındadır (Çoban, 2020'den).*

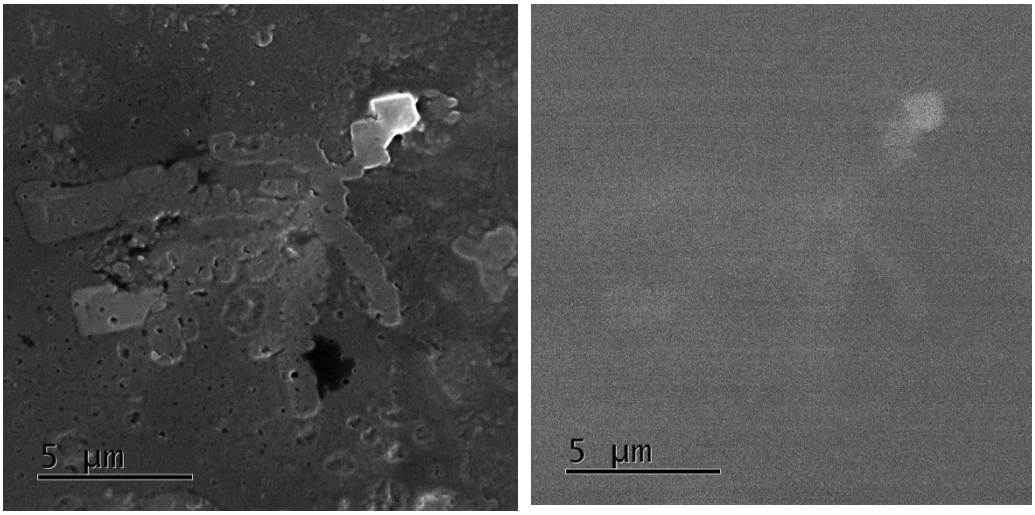

Figure 10. SE (left) and CL overlay (right) images of the Seydiler opal sample. Although the CL signal appears visually weak, localized bright domains (right) correspond to Mn-enriched microzones). These observations support trace-level cathodoluminescence activity related to Mn^{2+} activation.

Şekil 10. *Seydiler opal örneğinin SE (sol) ve CL kaplama (sağ) görüntüleri. CL sinyali görsel olarak zayıf görünse de, yerel parlak alanlar (sağ) Mn ile zenginleştirilmiş mikro bölgelere karşılık gelmektedir. Bu gözlemler, Mn^{2+} aktivasyonuyla ilişkili eser düzeyde katodolüminesans aktivitesini desteklemektedir.*

opal-CT and minor opal-C without the influence of hydrothermal systems.

Cathodoluminescence

Cathodoluminescence (CL) imaging and RGB compositional mapping were used to investigate the nanoscale heterogeneity and internal growth features of Seydiler opals. The SE-CL overlay image (Figure 9) reveals weak but detectable luminescence signals in a few localized domains. Although visually subtle, these features are spectrally supported by a well-defined Mn^{2}+-related luminescence peak around ~660 nm, confirming the presence of CL activity at a microdomain level, in a few isolated zones. These regions coincide with texturally distinct zones and may correspond to areas of trapped organics or Fe/Mn-bearing subdomains.

A broad optical emission spectrum (Figure 11) collected from the same region displays a dominant luminescence peak centered around ~640–670 nm, within the deep red portion of the visible range. This peak is characteristic of Mn^{2+}-activated cathodoluminescence, likely linked to tetrahedrally coordinated Mn in the opal structure. Additional weaker shoulders at ~780 and ~880 nm may indicate the presence of minor Fe^{3+} activators or defect-related emissions. Such luminescence behavior strongly supports the presence of Mn^{2+} substitution or nano-clustering within the silica network. It further confirms that the dendritic and microzonally enriched Mn observed in SEM is structurally integrated rather than surface-adsorbed.

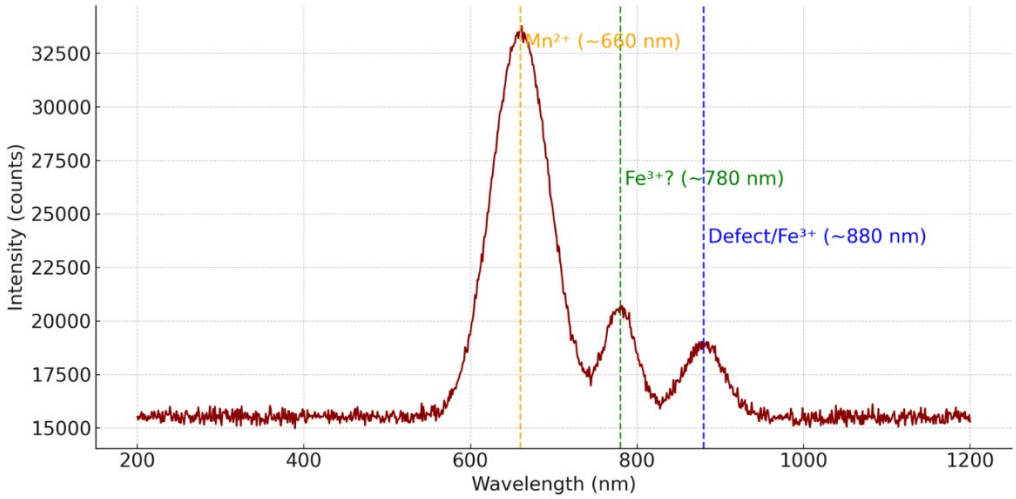

Figure 11. CL spectrum of the Seydiler opal shows a dominant Mn^{2+} emission at ~660 nm, with additional peaks at ~780 nm and ~880 nm attributed to Fe^{3+} and defect-related centers. These confirm localized luminescence despite overall weak CL contrast.

Şekil 11. *Seydiler opalinin CL spektrumu, ~660 nm'de baskın bir Mn^{2+} emisyonu göstermektedir; ayrıca ~780 nm ve ~880 nm'de Fe^{3+} ve kusurla ilişkili merkezlere atfedilen ek tepe noktaları bulunmaktadır. Bunlar, genel olarak zayıf CL kontrastına rağmen lokalize lüminesansı doğrulamaktadır.*

FT-IR spectroscopy studies

The FT-IR spectra of representative Seydiler diatomite samples indicate that the ooze unit is dominated by hydrous, amorphous, and poorly ordered silica phases, consistent with biogenic opal-A derived from diatom frustules (Figure 12). A broad absorption between ~3450–3350 cm^{-1} reflects O–H stretching, associated with both molecular water and structurally bound hydroxyl groups. This is accompanied by a band near ~1640 cm^{-1}, attributed to H–O–H bending vibrations of water retained in the silica matrix, a hallmark of diatomaceous opal-A. The spectra also show a strong, broad band around 1050–1100 cm^{-1} due to asymmetric Si–O–Si stretching, and weaker bands near 470–450 cm^{-1} corresponding to Si–O–Si bending. These features confirm the presence of a hydrated, amorphous opaline silicate framework (Taylor et al., 1970; Stockton & Fritsch, 1987; Yamagishi et al., 1997).

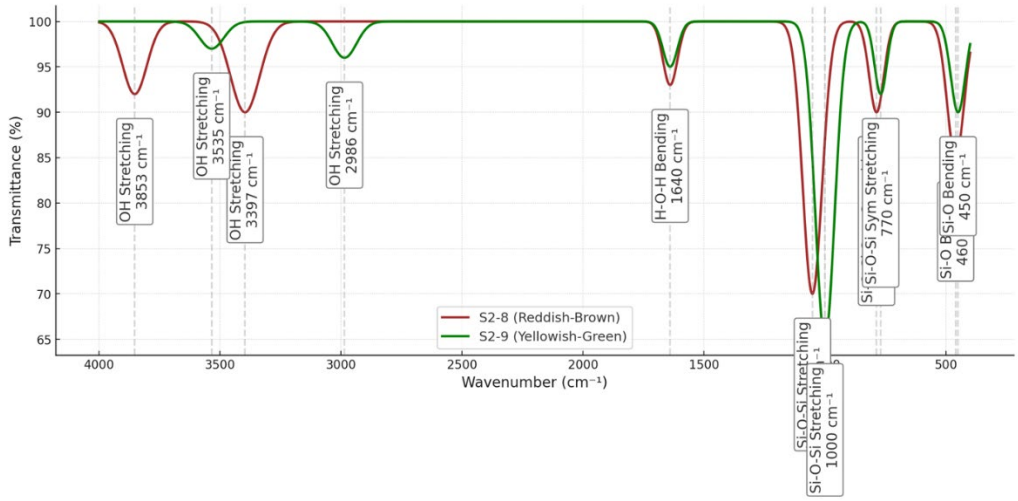

Figure 12. The simulated FT-IR spectra of S2-8 and S2-9 opal samples show characteristic OH and Si–O–Si vibrational bands indicative of hydrated opal-CT structure.

Şekil 12. *S2-8 ve S2-9 opal örneklerinin simüle edilmiş FT-IR spektrumları, hidratlı opal-CT yapısının göstergesi olan karakteristik OH ve Si–O–Si titreşim bantlarını göstermektedir.*

All three diatomite samples display spectral characteristics consistent with unaltered opal-A, indicating minimal diagenetic modification and preservation of their original biogenic structure. The combination of broad OH features, strong Si–O vibrational bands, high SiO_2 content (82–86%), and low Al_2O_3–Fe_2O_3 levels supports the purity and biogenic origin of the siliceous ooze. Under mild burial conditions, these conditions represent an ideal precursor for subsequent opal-CT transformation during early diagenesis.

The FT-IR spectra of Seydiler diatomites reveal that the ooze unit is predominantly composed of hydrous, amorphous, and poorly ordered silica phases, typical of biogenic opal-A derived from diatomaceous sources (Figure 13). These spectra exhibit diagnostic vibrational bands consistent with diatom frustule-derived silica deposited in low-temperature lacustrine environments. A broad absorption band between ~3450–3350 cm-¹ corresponds to O–H stretching vibrations, indicating the presence of both molecular water and structurally bound hydroxyl groups within the opaline matrix. This is accompanied by a distinct absorption near ~1640 cm-¹, attributed to the H–O–H bending mode of molecular water retained in the silica network. These hydrous features are characteristic of biogenic opal-A and are commonly associated with diatomaceous materials (Iler, 1979; Yamagishi et al., 1997).

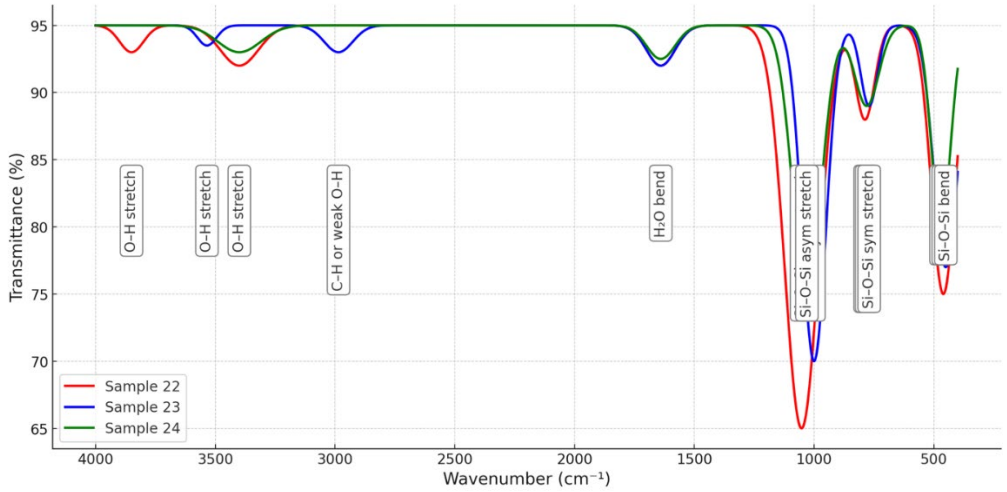

Figure 13. Simulated FT-IR transmittance spectra of diatomite samples (sample 22 (UL), 23, (ML) and 24(LL)) from the Seydiler ooze unit, showing broad OH–H_2O bands (3850–3400 and ~1640 cm-¹) and strong Si–O–Si stretching near 1050 cm-¹. The spectral features are typical of biogenic, amorphous opal-A, indicating low-temperature, early diagenetic silica formed from diatom frustules.

Şekil 13. *Seydiler ooze biriminden alınan diatomit örneklerinin (örnek 22 (UL), 23, (ML) ve 24(LL)) simüle edilmiş FT-IR geçirgenlik spektrumları, geniş OH–H_2O bantları (3850–3400 ve ~1640 cm-¹) ve 1050 cm-¹ civarında güçlü Si–O–Si gerilmesi göstermektedir. Spektral özellikler, diatom früstüllerinden oluşan düşük sıcaklıktaki, erken diyajenetik silikayı gösteren biyojenik, amorf opal-A'nın tipik özellikleridir.*

The dominant, broad band centered near 1050–1100 cm-¹ corresponds to asymmetric Si–O–Si stretching vibrations, confirming the presence of an opaline silicate framework. Additionally, weaker peaks observed around ~470–450 cm-¹ are linked to Si–O–Si bending modes, further supporting the identification of hydrated, amorphous opaline silica (Taylor et al., 1970; Flörke et al., 1991). The spectral profiles of all three samples are consistent with opal-A rather than more ordered opal-CT, suggesting that the diatomite layers have undergone minimal diagenetic alteration and retain their original biogenic silica structure.

Moreover, the broad O–H stretching bands and well-defined Si–O features in the Seydiler samples suggest favorable precursor conditions for subsequent opal-CT transformation under mild burial and early diagenetic processes. When combined with high SiO_2 content (82–86%) and relatively low Al_2O_3 and Fe_2O_3 levels from XRF data, these results reinforce the biogenic origin and purity of the siliceous ooze, confirming its role as a significant source material for opal formation in the Seydiler deposit.

Raman spectroscopy studies

The Raman spectra of Seydiler opals exhibit characteristic vibrational bands of partially ordered opaline silica, confirming the coexistence of pseudo-crystalline opal-CT and transitional opal-C phases (Figure 14). These phases are interpreted as low-temperature diagenetic derivatives of a biogenic opal-A precursor. In the low-wavenumber region

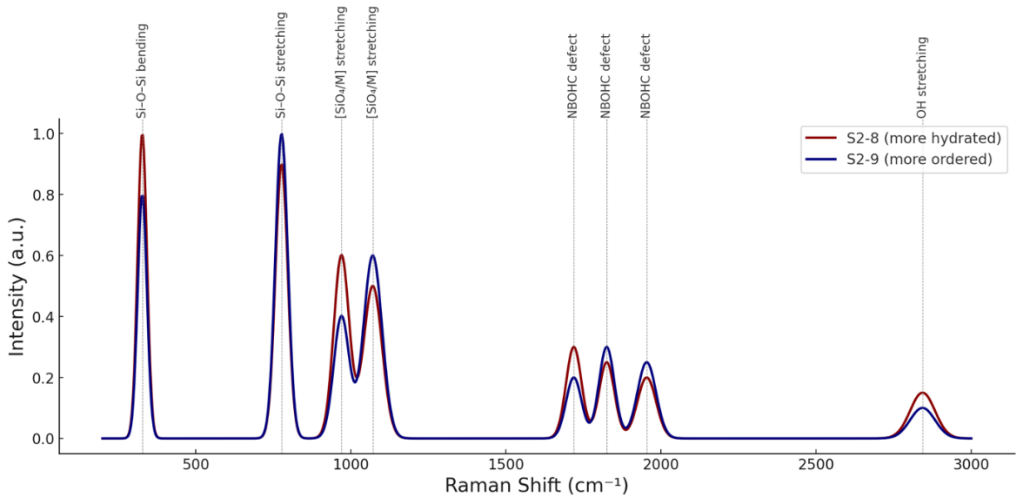

Figure 14. Simulated representative Raman spectra of Seydiler opal samples (S2-8 and S2-9), showing key vibrational bands of partially ordered opaline silica, including Si–O–Si bending (~328 cm-¹), stretching (~777 cm-¹), trace element-related [SiO_4/M] modes (~970–1071 cm-¹), NBOHC defects (~1719–1954 cm-¹), and OH-stretching (~2843 cm-¹).

Şekil 14. *Seydiler opal örneklerinin (S2-8 ve S2-9) simüle edilmiş temsili Raman spektrumları, kısmen düzenli opalin silikanın temel titreşim bantlarını göstermektedir; bunlar arasında Si–O–Si bükülmesi (~328 cm-¹), gerilme (~777 cm-¹), eser elementle ilişkili [SiO_4/M] modları (~970–1071 cm-¹), NBOHC kusurları (~1719–1954 cm-¹) ve OH gerilmesi (~2843 cm-¹) yer almaktadır.*

(200–800 cm-¹), peaks at ~328 cm-¹ (Si–O–Si bending) and ~777 cm-¹ (symmetric Si–O–Si stretching) reflect progressive silica ordering from opal-A to opal-CT and localized opal-C domains (Kingma & Hemley, 1994; Colomban & Prinsloo, 2009). The mid-wavenumber region (~900–1100 cm-¹) features bands at ~970 and ~1071 cm-¹, attributed to [SiO_4/M] tetrahedral vibrations, where M includes cations such as Fe, Zn, Cs, and U. These shifts align with trace-element incorporation observed in geochemical data, suggesting early diagenetic cation substitution (McCreery, 2005). Higher wavenumber bands at ~1719, ~1825, and ~1954 cm-¹ are linked to non-bridging oxygen hole centers (NBOHCs), indicating structural defects from post-depositional reorganization. A minor ~2843 cm-¹ band may correspond to isolated OH vibrations.

These spectral features collectively support a biogenic opal-A transformation into opal-CT, accompanied by minor opal-C development, which is governed by low-temperature diagenesis and trace-element interactions.

Geochemistry

Major, trace, and rare earth element geochemistry

Chemical analyses of two representative Seydiler opal samples (S2-8 and S2-9) reveal high silica content (94.53 wt.% and 93.61 wt.%) (Table 1) and distinct trace element signatures, consistent with formation in a lacustrine, diatomite-rich depositional environment. Both samples exhibit low concentrations of major oxides, including Al_2O_3, Fe_2O_3, and CaO. S2-8 sample is slightly enriched in Fe_2O_3 (0.68%) and CaO (0.16%), aligning with its reddish-brown color. In contrast, S2-9 contains more Al_2O_3 (0.18%), suggesting the presence of minor aluminosilicate phases, such as clays or feldspars. Loss on ignition (LOI) values of 4.5% (S2-8) and 5.5% (S2-9) indicate retained structural water and hydroxyl groups, characteristic of hydrous opaline silica ($SiO_2 \cdot nH_2O$).

These concentrations surpass the typical values reported for global sedimentary opals, suggesting biogenic uptake by diatoms and secondary enrichment from remote Neogene volcanic ash layers.

S2-8 also indicates elevated levels of Be (13 ppm), As (23.2 ppm), Pb (2.6 ppm), and Hg (3.45 ppm), which may suggest the presence of Fe-oxide microenvironments or organic associations. In contrast, S2-9 is enriched in U (97.4 ppm), Cs, and Zr (5.3 ppm) (Table 1), potentially linked to early diagenetic trace-element substitution or minor volcanic influence. Both samples reveal negligible concentrations of heavy metals, such as Cd, Sb, and Bi, while rare earth elements (e.g., La, Ce, Nd) are present at low levels, with slightly higher values in S2-9. These patterns indicate a low-temperature, non-hydrothermal diagenetic environment for opal formation, characterised by localised redox variation and trace element mobilisation. Major oxide data from three stratigraphic levels lower (LL), middle (ML), and upper (UL) from diatomite deposit indicate a progressive enrichment in silica content up-section, with SiO_2 increasing from 82.19 wt. (LL) to 85.07 wt. (ML) and peaking at 86.22 wt. (UL) (Table 2). This trend reflects enhanced biogenic input from diatoms and a decrease in detrital dilution, consistent with the transition to more isolated lacustrine conditions in the upper stratigraphy. Meanwhile, Al_2O_3 and Fe_2O_3 contents decline (Al_2O_3: 5.14% → 2.20%; Fe_2O_3: 1.46% → 0.62%), indicating a reduced supply of aluminosilicate and iron-bearing phases. These changes support a low-energy depositional environment conducive to the preservation of amorphous silica.

CaO concentrations increase toward the top of the sequence (1.08% in UL), potentially signaling localized carbonate contributions or early diagenetic calcite precipitation. MgO, K_2O, and Na_2O occur in low concentrations, reflecting minimal feldspar or clay input. Minor oxides, such as TiO, MnO, SrO, and ZrO_2, appear in lower amounts and may be linked to volcanic ash admixture or evaporitic influences. SO_3 is present throughout the profile (0.06–0.18%), suggesting diagenetic incorporation of sulfate minerals. Notably, NiO, ZnO, and BaO are more prominent in the lower and middle levels, indicating localized elemental enrichment that may be tied to microbial processes or transient hydrothermal episodes.

Oxygen isotope geochemistry of Seydiler Opals

This study measured the $\delta^{18}O$ values of two representative opal samples, yielding average values of 24.40‰ and 25.03‰, respectively (Table 3). These isotopically enriched compositions indicate precipitation from a meteoric water-influenced environment. The $\delta^{18}O$ values of meteoric waters in the Seydiler region generally range from −11.5‰ to −7.5‰

Table 1. The results of major, trace, and rare earth elements analyses of the representative opals from the Seydiler region.

Tablo 1. *Seydiler yöresindeki temsili opallerin majör, eser ve nadir toprak element analiz sonuçları.*

Major oxides (%)												
Sample	**SiO_2**	**Al_2O_3**	**Fe_2O_3**	**MgO**	**CaO**	**Na_2O**	**K_2O**	**TiO_2**	**P_2O_5**	**MnO**	**Cr_2O_3**	**LOI**
S2-8	94,53	0,09	0,68	0,01	0,07	0,02	0,03	<0,01	<0,01	<0,01	<0,002	4,5
S2-9	93,61	0.18	0,36	0,02	0,16	0,02	0,04	<0,01	<0,01	0,01	<0,002	5,5
Trace and rare earth elements (ppm), Au(ppb)												
S2-8	**Ba**	**Ni**	**Sc**	**Be**	**Co**	**Cs**	**Ga**	**Hf**	**Nb**	**Rb**	**Sn**	**Sr**
	31	<20	<1	13	0,5	49,8	<0,5	<0,1	1,1	8	<1	7,4
	Ta	**Th**	**U**	**V**	**W**	**Zr**	**Y**	**La**	**Ce**	**Pr**	**Nd**	**Sm**
	<0,1	<0,2	2,9	<8	0,6	3,7	0,4	0,4	0,2	0,03	<0,3	<0,05
	Eu	**Gd**	**Tb**	**Dy**	**Ho**	**Er**	**Tm**	**Yb**	**Lu**	**Mo**	**Cu**	**Pb**
	<0,02	0,06	<0,01	0,07	<0,02	0,04	<0,01	0,06	<0,01	1,4	5	2,6
	Zn	**Ni**	**As**	**Cd**	**Sb**	**Bi**	**Ag**	**Au**	**Hg**	**Tl**	**Se**	
	671	2,4	23,2	<0,1	1,2	<0,1	<0,1	1,2	3,45	0,1	<0,5	
S2-9	**Ba**	**Ni**	**Sc**	**Be**	**Co**	**Cs**	**Ga**	**Hf**	**Nb**	**Rb**	**Sn**	**Sr**
	20	<20	<1	6	0,2	78,6	<0,5	0,1	0,6	10,9	<1	11,9
	Ta	**Th**	**U**	**V**	**W**	**Zr**	**Y**	**La**	**Ce**	**Pr**	**Nd**	**Sm**
	<0,1	0,3	97,4	<8	0,6	5,3	0,1	0,5	0,7	0,05	<0,3	<0,05
	Eu	**Gd**	**Tb**	**Dy**	**Ho**	**Er**	**Tm**	**Yb**	**Lu**	**Mo**	**Cu**	**Pb**
	<0,02	<0,05	<0,01	<0,05	<0,02	0,03	<0,01	0,05	<0,01	0,8	4,6	0,5
	Zn	**Ni**	**As**	**Cd**	**Sb**	**Bi**	**Ag**	**Au**	**Hg**	**Tl**	**Se**	
	999	0,2	0,7	<0,1	0,6	<0,1	<0,1	1,5	0,13	<0,1	<0,5	

Table 2. The results of major and minor element analysis by XRF for the Seydiler diatomites

Tablo 2. *Seydiler diatomitleri için XRF ile yapılan majör ve minör element analiz sonuçları*

%	Upper level (UL)	Middle level (ML)	Lower lev (LL)
SiO_2	86.22	85.07	82,19
Al_2O_3	2,20	2,81	5,14
Fe_2O_3	0,62	1,27	1,46
CaO	1,08	0,59	0,64
K_2O	0,15	0,09	0,23
MgO	0,31	0,39	0,37
Na_2O	0,17	-	0,31
TiO_2	0,16	0,09	0,12
MnO	0,02	-	0,02
SrO	0,01	0,02	0,02
ZrO_2	0,01	-	0,01
Cl	0,05	0,07	0,04
SO_3	0,11	0,18	0,06
NiO	-	0,02	-
ZnO	-	0,05	0,01
BaO	-	-	0,10

(Kolodny & Epstein, 1976; Aksever et al., 2018; Başaran, 2017), which aligns with Miocene paleoprecipitation estimates for central-western Anatolia (Yıldırım et al., 2021).

The silica–water oxygen isotope fractionation equation proposed by Chauviré et al. (2019) was employed to determine formation temperatures. Using the measured $\delta^{18}O$ values of opal and assuming meteoric water $\delta^{18}O$ values of −11.5‰ and −7.5‰, the corresponding precipitation temperatures were calculated with a precision of 0.1 °C. These calculated temperatures fall within the known stability ranges for opal-CT and transitional opal-C phases, typically between 30 °C and 80 °C (Hein et al., 1978). Specifically, the Seydiler opals formed within a temperature range of 31.3°C to 50.9°C, as shown in Figure 15.

Table 3. Calculated formation temperatures (°C) for Seydiler opals based on individual $\delta^{18}O$ (V-SMOW) values, using the silica–water fractionation model by Chauviré et al. (2019) under two meteoric water $\delta^{18}O$ scenarios (–11.5‰ and –7.5‰).

Tablo 3.*Chauviré ve ark. (2019) tarafından geliştirilen silika-su fraksiyonlaşma modelini kullanarak, iki meteorik su $\delta^{18}O$ senaryosu (–11,5‰ ve –7,5‰) altında, Seydiler opalleri için hesaplanan oluşum sıcaklıkları (°C).*

Sample	$\delta^{18}O$ (‰)	Water $\delta^{18}O$ (‰)	Temperature (°C)
S2-8_1	24.67	–11.5	32.4
		–7.5	50.0
S2-8_2	24.68	–11.5	32.3
		–7.5	49.9
S2-8_3	23.86	–11.5	35.2
		–7.5	52.8
Avg (S2-8)			**33.3 / 50.9**
S2-9_1	25.09	–11.5	31.2
		–7.5	48.8
S2-9_2	24.71	–11.5	32.6
		–7.5	50.1
S2-9_3	25.29	–11.5	30.2
		–7.5	47.8
Avg (S2-9)			**31.3 / 48.9**

Sample S2-8 yielded formation temperatures between 32.3 °C and 50.9 °C, while S2-9 ranged from 31.3 °C to 48.9 °C. These values are consistent with early-stage burial diagenesis and low-temperature silica precipitation. The observed opaline

mineralogy, dominated by pseudo-crystalline opal-CT and minor transitional opal-C, is consistent with previous reports on the transformation of biogenic opal-A under similar thermal regimes. According to Jones and Segnit (1971) and Hesse (1988), the transition from amorphous opal-A to opal-CT commonly occurs within the temperature range of ~30–50 °C during shallow burial.

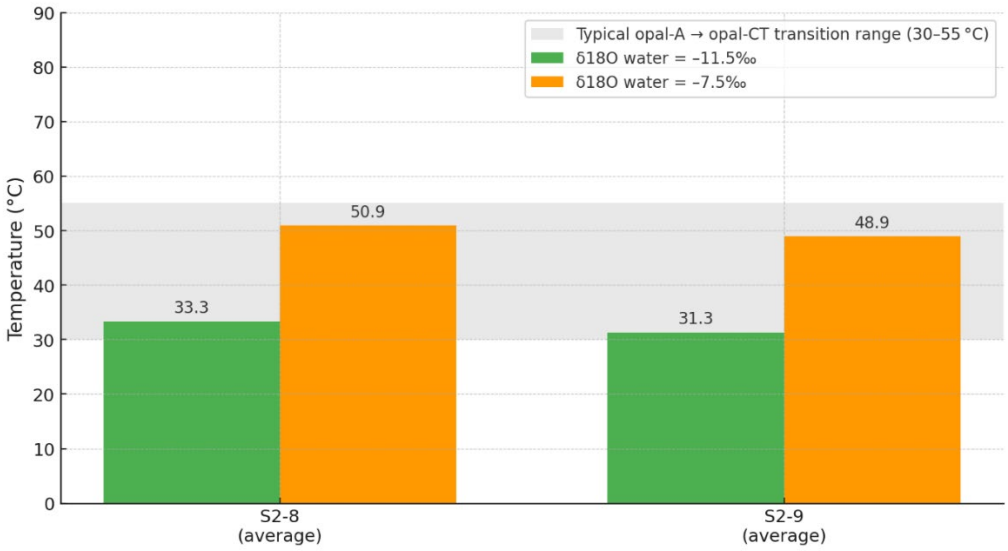

Figure 15. Estimated formation temperatures of Seydiler opal samples (S2-8 and S2-9), calculated from δ¹⁸O values using the silica–water oxygen isotope fractionation equation proposed by Chauviré et al. (2019). Two δ¹⁸O(water) scenarios (–11.5‰ and –7.5‰ V-SMOW) reflect the presence of Miocene meteoric fluids. The shaded band (30–55 °C) represents the typical diagenetic transition zone from opal-A to opal-CT, consistent with burial-driven silica ordering under suboxic, lacustrine conditions.

Şekil 15. *Seydiler opal örneklerinin (S2-8 ve S2-9) tahmini oluşum sıcaklıkları, Chauviré ve diğ. (2019) tarafından önerilen silika-su oksijen izotop fraksiyonlaşma denklemi kullanılarak δ¹⁸O değerlerinden hesaplanmıştır. İki δ¹⁸O(su) senaryosu (–11,5‰ ve –7,5‰ V-SMOW), Miyosen meteorik sıvılarının varlığını yansıtmaktadır. Gölgeli bant (30–55°C), suboksik, gölsel koşullar altında gömülmeyle yönlendirilen silika düzeniyle tutarlı olarak, opal-A'dan opal-CT'ye tipik diyajenetik geçiş bölgesini temsil eder.*

Lu et al. (2020) further support that such low-temperature transformations significantly influence pore structure development in siliceous shales. These findings are corroborated by Williams and Crerar (1985), who emphasized that more advanced transformations, such as the conversion of opal-CT to microcrystalline quartz, generally require higher temperatures exceeding 60–80 °C conditions not evidenced in the Seydiler Basin. Therefore, the isotopic temperature data and mineralogical assemblages jointly indicate a non-hydrothermal, biogenic opal formation process driven by low-temperature diagenesis within a lacustrine, meteoric-fluid–dominated environment.

Gemological characteristics of the Seydiler Opals

The Seydiler opals, classified as hydrous opaline-quartz varieties ($SiO_2 \cdot nH_2O$), exhibit physical and optical characteristics consistent with their biogenic and diagenetic origin. Specific gravity values range from 2.18 to 2.30 (Table 4), typical of sedimentary opals with high silica content and minor enrichments in trace elements, such as Zn, Cs, and U. The refractive index (n ≈ 1.451) corresponds to pseudo-crystalline opal-CT and transitional opal-C phases. These opals exhibit natural, untreated coloration ranging from reddish-brown to yellowish-green, characterized by a vitreous to waxy luster and a translucent to transparent diaphaneity. Their hydrous nature, however, makes them susceptible to dehydration-related surface crazing or internal fracturing following extraction. Stabilisation may be necessary to ensure long-term durability and maintain gem quality.

With a Mohs hardness of ~5.5, compact fracture surfaces, and isotropic microcrystalline texture, Seydiler opals meet several key criteria for gem-quality classification. Their optical clarity, vibrant zoning, and structural integrity underscore their significance among sedimentary-origin opals that lack play-of-color.

Raw gem-quality opal samples selected as representatives were cut, polished, and processed into various jewellery forms, including cabochons and free-form polished stones (Figure 16). These operations demonstrated that the Seydiler opals possess sufficient mechanical integrity, surface coherence, and aesthetic appeal to be utilized as gemstones. Unlike many sediment-hosted opals that are highly porous or friable, Seydiler opals show a degree of cohesion and homogeneity that allows lapidary shaping and polishing without significant fracturing or loss of material.

Table 4. Some essential gemological properties of the Seydiler gemmy opals.

Tablo 4. *Seydiler mücevher opallerinin bazı temel gemolojik özellikleri.*

Basic Gemological Measurements	Seydiler Gem Opals
Specific gravity (SG)	S.G.= 2.18-2.30
Optical character	Isotropic, micro-crystalline
Refractive index (RI)	Nε-ω=1.450
Luminescence against UV excitation	Inert
Cleavage	None
Fracture	Flat surfaces (not cleavage) fractured in conchoidal pattern
Diaphaneity	Transparent to translucent
Hardness	5.5 (approximately)
Luster	Vitreous

The sample shown in Figure 16 displays a semi-transparent to translucent structure with vibrant orange to amber hues, suggesting the presence of iron oxides as chromophoric agents. Following mechanical processing, the resulting gemstone (Figure 17) exhibits a smooth, lustrous surface with internal patterning and color zoning, enhancing its visual appeal. Such characteristics highlight the unique potential of Seydiler opals for use in gem-quality applications.



Figure 16. Raw gem-quality opal from the Seydiler region. This unprocessed opal specimen displays a semi-transparent to translucent appearance with rich amber-to-rust coloration. The internal color zoning and natural surface luster indicate high visual quality and minimal porosity, making it suitable for ornamental use.

Şekil 16*. Seydiler bölgesine ait ham süstaşı kalitesinde opal örneği. İşlenmemiş bu opal örneği, yarı saydamdan saydama geçiş gösteren yapısıyla kehribar ve pas tonlarında zengin renklenme sunmaktadır. İçsel renk zonlanması ve doğal yüzey parlaklığı, görsel kalitesinin yüksekliğini ve düşük gözenekliliğini göstererek süstaşı kullanımına uygunluğunu vurgulamaktadır.*

These findings confirm that opals formed under low-temperature, diagenetically controlled, biogenic–lacustrine conditions can reach the quality standards required for gemstone processing. Thus, the Seydiler deposit is not only of mineralogical and genetic significance but also holds promise for economic use in artisanal or regional jewellery production, especially considering the ease of local processing and polishing.



Figure 17. Polished Seydiler opal prepared for jewellery application. After cutting and polishing, the specimen shows a smooth surface with intense color saturation and visual coherence. The cabochon form exhibits minimal fracturing, indicating excellent mechanical integrity and lapidary compatibility.

Şekil 17*. Takı üretimi için işlenmiş ve parlatılmış Seydiler opali. Kesme ve cilalama işlemleri sonrasında örnek, düzgün yüzeyi, yoğun renk doygunluğu ve görsel bütünlüğü ile dikkat çekmektedir. Kabaşon formunda şekillendirilen taşta belirgin kırık izlerine rastlanmaması, yüksek mekanik bütünlük ve taş işçiliğine uygunluk göstermektedir.*

DISCUSSION

The Seydiler opal deposit offers a representative model of early-stage silica diagenesis in a non-marine, biogenically enriched lacustrine environment. Mineralogical analyses, particularly XRD, FTIR, and Raman spectroscopy, reveal that the transformation of amorphous biogenic opal-A to pseudo-crystalline opal-CT and incipient opal-C occurred under shallow burial conditions and low temperatures, typically within the 30–50 °C range. These observations are consistent with

previously established transformation windows for biogenic opal (Jones & Segnit, 1971; Hesse, 1988).

Stable oxygen isotope values further constrain formation temperatures between ~31 and 51°C, supporting early diagenetic restructuring without progressing to high-temperature phases, such as microcrystalline quartz. The rare presence of α-quartz, interpreted exclusively as detrital inclusions possibly sourced from volcanic ash, reinforces the absence of advanced recrystallisation (>70–80 °C), as noted in other lacustrine systems (Williams & Crerar, 1985).

Variations in structural ordering between samples (e.g., S2-9 vs. S2-8) likely reflect microenvironmental heterogeneities such as pore fluid composition, compaction intensity, and localized ionic activity. S2-9 exhibits sharper and more defined opal-CT peaks, indicative of advanced ordering, whereas S2-8 retains broader features, suggesting residual opal-A. Minor calcite occurrences, associated with peaks at d = 3.03 Å and 2.28 Å, indicate co-diagenetic carbonate precipitation under slightly alkaline, Ca-rich conditions, likely facilitated by volcaniclastic alteration (e.g., plagioclase breakdown).

High-resolution SEM images reveal the abundance of well-preserved diatom frustules, belonging to taxa such as Ellerbeckai sp., Gomphonema, sp. and Halamphora sp., as well as newly recorded species (Staurosirella pinnata morphotypes 3 and 6), indicating high primary productivity. These biological inputs served as the principal silica source. Similar biogenic enrichments and well-preserved frustules have been reported in other lacustrine diatomite deposits such as Lake Abiyata (Ethiopia) (Hunegnaw & Getaneh, 2024), Ihlara–Selime (Türkiye) (Gürel & Yıldız, 2006), Karacaören–Nevşehir (Yıldız et al., 2017), and La Pampa (Argentina) (Fayó et al., 2025). These analogues exhibit transformation sequences from opal-A to opal-CT within comparable temperature windows (30–50 °C) and shallow burial depths. The presence of Fe–Mn oxides, halite microcrystals, and enrichments in Zn, Cs, Rb, and U support a scenario involving periodic evaporation, microbial mediation, and redox-sensitive mobilization in a confined, semi-evaporitic basin. Comparable signatures were detected in other volcanic–lacustrine diatomites where hydrothermal input was minimal, and biogenic silica was preserved in high abundances (e.g., Hunegnaw & Getaneh, 2024; Gürel & Yıldız, 2007).

Considering the Western Anatolian extensional domain's high geothermal gradient (40–50°C/km), the opal-CT transformation depth (~880 m) aligns well with regional burial models. Overall, the Seydiler deposit exemplifies a non-hydrothermal, biologically mediated opalization process, representing an essential analogue for early silica diagenesis in continental settings.

CONCLUSIONS

The Seydiler opal deposit in the northeastern part of Afyonkarahisar (western Türkiye) represents a rare stratiform, gem-quality opal formation in a non-marine, Miocene lacustrine environment. Hosted within a volcano-sedimentary succession composed of interbedded diatomite, tuffite, and siliceous ooze, the opals originated through the low-temperature transformation of biogenic opal-A into structurally ordered opal-CT and minor incipient opal-C.

XRD, FTIR, and Raman analyses confirm the dominance of pseudo-crystalline opal-CT, with spectroscopic features including Si–O–Si stretching and bending (~777 cm^{-1}, ~328 cm^{-1}), and OH–H_2O absorption (~3400, 1640 cm^{-1}). Detected α-quartz is present solely as a detrital inclusion, rather than a diagenetic product.

Scanning electron microscopy (SEM) observations reveal exceptionally well-preserved siliceous frustules belonging to a diverse diatom assemblage. The identified taxa include representatives of the genera Ellerbeckia sp., Gomphonema sp., Pinnularia sp., Halamphora sp., and Staurosira sp.. In addition, newly recorded morphotypes of Staurosirella pinnata (morphotypes 3 and 6) have been documented for the first time in this deposit. The abundance, taxonomic diversity, and high degree of morphological preservation of these frustules collectively indicate intense primary productivity and a predominantly biogenic origin for the precursor silica.

Geochemically, the opals are enriched in Zn, Cs, Rb, and U, reflecting a combination of biological uptake and volcaniclastic sediment input. Minor calcite formation is associated with the release of Ca from altered ash layers and early-stage carbonate precipitation in slightly alkaline pore waters.

Isotopic thermometry based on $\delta^{18}O$ values (23.86–25.29‰ V-SMOW) yields formation temperatures between 31 °C and 51 °C. These estimates are consistent with the opal-A to opal-CT transition and confirm early-stage diagenesis. The absence of indicators for opal-CT to α-quartz conversion corroborates the low thermal evolution.

From a regional perspective, the basin's high geothermal gradient (~40–50 °C/km) and modeled burial depth (~880 m) are compatible with observed mineral transformations. Surface uplift and erosion subsequently exposed the opaline layers at shallow depths (3–5 m).

Gemologically, the Seydiler opals exhibit desirable characteristics, including vibrant natural colors, a vitreous to waxy luster, a refractive index (RI) of ~1.451, a specific gravity (SG) of 2.18–2.30, and a low inclusion density. However, high water content may lead to dehydration-related cracking, necessitating post-extraction stabilization.

The Seydiler deposit is a prime example of lacustrine opalization driven entirely by biogenic and sedimentary processes without hydrothermal influence. This makes it valuable not only as a gemstone source but also as a natural analogue for low-temperature silica diagenesis in closed-basin systems.

These properties confirm that opals formed under low-temperature, diagenetically controlled, biogenic lacustrine conditions can reach the quality standards required for gemstone processing. Thus, the Seydiler deposit is not only of mineralogical and genetic significance but also holds promise for economic use in artisanal or regional jewellery production, especially considering the ease of local processing and polishing.

The Seydiler gem-quality opals represent one of the rare, documented cases in the literature where gem-quality opals are derived directly from diatomaceous precursors in a non-marine setting. Unlike typical hydrothermal or volcanic-hosted opals, which are more commonly associated with precious opal formation, the Seydiler specimens demonstrate that early-stage burial diagenesis of biogenic silica (especially diatom frustules) can yield dense, cohesive, and aesthetically vibrant opal materials suitable for lapidary use. This makes the Seydiler opals a unique case study for gemological and sedimentological research, highlighting the potential of lacustrine diatomites to host economically valuable opal mineralization.

ACKNOWLEDGMENT

The paper is a part of "Characterization and Economic Potential of Gemstone Opals from Seydiler, Afyonkarahisar" doctoral thesis.

REFERENCES

Açıkalın, N. 1991. Türkiye'de ve dünyada diyatomit. MTA, F.E.D., 30 s. (in Turkish).

Akal, C., Helvacı, C., Prelevic, D., Van Den Bogard, P. 2013. High-K volcanism in the Afyon region, western Türkiye; from Si-oversaturated to Si-undersaturated volcanism. International Journal of Earth Sciences, 102, 435–453. DOI: 10.1007/s00531-012-0809-9

Aksever, F., Yığ, H., Bilgiç, S. 2018. Büyük Sincanlı (Sinanpaşa) ovası (Afyonkarahisar) su kaynaklarının hidrojeokimyasal değerlendirilmesi. Mühendislik Bilimleri ve Tasarım Dergisi, 6(2), 239–249. DOI: 10.21923/jesd.411182

Andolfato, U. 1969. Afyon ili mermer alanlarının ekonomik olanakları üzerine genel ve ayrıntılı araştırma, değerlendirme, teknoloji, rezerv ve sanayi durumu. MTA Rapor No:4281. (Unpublished, in Turkish).

Aydar, E., Bayhan, H., Gourgaud, H. 1998. Köroğlu caldera, mid-west Anatolia, Türkiye: volcanological and magmatological evolution. Journal of Volcanology and Geothermal Research, 85, 83–98. DOI: 10.1016/S0377-0273(98)00051-1

Bargu, S. 1991. İsçehisar-Bayat arası ile Paşadağın (Afyon) jeolojisi ve stratigrafisi. Yerbilimleri, 9(1–2), 14–36. https://icerik.maden.org.tr/uploads/portal/resimler/ekler/8cfbf77a3d250a4_ek.pdf

Başaran, M. 2017. Türkiye'deki opal oluşumlarının jeokimyasal ve mineralojik incelenmesi. İstanbul Üniversitesi, Yüksek Lisans Tezi, İstanbul

Bircan, A. 1968. Türkiye diyatomit envanteri. MTA Yayınları, No:138, 28 s. (in Turkish).

Candan, O., Çetinkaplan, M., Oberhänsli, R., Rimmele, G., Akal, C. 2005. Alpine High-P/Low-T metamorphism of the Afyonkarahisar Zone. Lithos, 84, 102–124. DOI: 10.1016/j.lithos.2005.02.005

Chauviré, B., Rondeau, B., Fritsch, E. 2019. The structure and chemistry of opal: A review. Mineralogical Magazine, 83(3), 351–373. DOI: 10.3390/min13030356

Colomban, P., Prinsloo, L. 2009. Optical spectroscopy of silicates and glasses. In: Yatwood J. et al. (eds.) Spectroscopic Properties of Inorganic and Organometallic Chemistry, RSC Publishing, 128–149. DOI: 10.1039/b715005a

Coradin, T., Lopez, P. J. 2003. Biogenic silica patterning: simple chemistry or subtle biology? ChemBioChem, 3, 1–9. DOI: 10.1016/j.crpv.2004.07.002

Çoban, E. 2020. Afyonkarahisar–Seydiler süstaşı opallerinin karakterizasyonu ve ekonomik potansiyeli. Kütahya Dumlupınar Üniversitesi, Fen Bilimleri Enstitüsü, Doktora Tezi, 133 s. (Unpublished).

Del Amo, Y., Le Pape, O., Tréguer, P. . 1997. Impacts of high-nitrate freshwater inputs. Marine Ecology Progress Series, 161, 213–224. DOI: 10.3354/meps161213

Easton, A. J., Joslin, I. E., Kempe, D. R. C., Hancock, J. M. 1982. Metasomatic alteration of pelagic ooze. Marine Geology, 48(1–2), M1–M8. DOI: 10.1016/0025-3227(82)90124-4

Ehrenberg, C. G. 1843. Verbreitung und Einfluss des mikroskopischen Lebens. Abhandlungen der Königlichen Akademie der Wissenschaften zu Berlin, 291–445.

Ergün, A. 1969. İscehisar (Afyon) ilçesi, Seydiler kasabası Hasan Abdullah Gediği diyatomit etüdü. MTA Rapor No:5125, 15 s. (Unpublished).

Fayó, R., Espinosa, M. A., Vélez-Agudelo, C. A. 2025. Paleoenvironmental reconstruction of a Neogene diatomite deposit. Geobios, 88–89, 91–101. DOI: 10.1016/j.geobios.2024.02.009

Finkel, Z. V., Benjamin, K. 2010. Silica use through time. Geomicrobiology Journal, 27, 596–608. DOI: 10.1080/01490451003702941

Flörke, O. W., Graetsch, H., Martin, B., Roller, K., Wirth, R. 1991. Nomenclature of micro- and non-crystalline silica minerals. Neues Jahrbuch für Mineralogie, 163, 19–42.

Fuhrmann, T., Landwehr, S., Rharbi-Kucki, M. E., Sumper, M. 2004. Diatoms as living photonic crystals. Applied Physics B, 78, 257–260. DOI: 10.1007/s00340-004-1419-4

Gürel, A., Yıldız, A. 2007. Diatom communities. Journal of Asian Earth Sciences, 30(1), 170–180. DOI: 10.1016/j.jseaes.2006.07.015

Hein, J. R., Scholl, D. W., Barron, J. A., . 1978. Diagenesis of late Cenozoic diatomaceous deposits. Sedimentology, 25, 155–181. DOI: 10.1111/j.1365-3091.1978.tb00307.x

Herve, V., Derr, J., Douady, S. . 2012. pH-dependence of silicon biomineralization. PLoS ONE, 7(10): e46722. DOI: 10.1371/journal.pone.0046722

Hesse, R. 1988. Origin of chert. Geoscience Canada, 15, 171–192. https://id.erudit.org/iderudit/geocan15_3art01

Hoek, C., Mann, D., Jahns, H. M. 1995. Algae: An Introduction to Phycology. Cambridge Univ. Press, 285 s.

Hunegnaw, Y., Getaneh, W. 2024. Geology, mineralogy, geochemistry. Heliyon, 10, e36132. DOI: 10.1016/j.heliyon.2024.e36132

Işık, I. 1984. Diyatomit. Anadolu Univ. Press, 81–98.

Iler, R. K. 1979. The Chemistry of Silica. John Wiley, New York, 730–801.

Jones, L. H. P., Segnit, E. R. 1971. The nature of opal I. Journal of the Geological Society of Australia, 18(1), 57–68.

Kingma, K. J., Hemley, R. J. 1994. Raman spectroscopic study of microcrystalline silica. American Mineralogist, 79, 269–273.

Kolodny, Y., Epstein, S. 1976. Stable isotope geochemistry of deep-sea cherts. Geochimica et Cosmochimica Acta, 40, 1195–1209.

Kröger, N. 2007. Prescribing diatom morphology. Current Opinion in Chemical Biology, 11, 662–669. DOI: 10.1016/j.cbpa.2007.10.009

Kuşcu, M., Yıldız, A. 2001. Ayazini (Afyon) tüflerinin yapı taşı. 3rd Marble Symposium of Turkey, Afyonkarahisar, 85–98.

Kuşcu, M., Bağcı, M., Yıldız, A. 2006. Konarı (İscehisar-Afyon) traki-andezitlerinin yapıtaşı olarak kullanılabilirliği. MARBLE 2006, 281–291.

Lange-Bertalot, H., Hofmann, G., Werum, M., Cantonati, M. 2017. Freshwater Benthic Diatoms of Central Europe. Koeltz Botanical Books, 942 s.

Lu, L., Liu, W., Yu, L. . 2020. Early diagenesis of biogenic opal. Petroleum Geology & Experiment, 42(3), 363–370.

McCreery, R. L. 2005. Raman Spectroscopy for Chemical Analysis. John Wiley & Sons, 448 s.

Medlin, L. K. 2009. Opinion: The use of centric and pennate. Diatom Research, 24, 499–501.

Metin, S., Genç, Ş., Bulut, V. 1987. Afyon ve dolayının jeolojisi. MTA Rapor No:2113, 74 s.

Okay, A. I. 1984. Kuzeybatı Anadolu'da yer alan metamorfik kuşaklar. Ketin Sempozyumu, Ankara, 83–92.

Özdamar, Ş., Billor, M. Z., Sunal, G.. 2013. First U-Pb SHRIMP zircon. Gondwana Research, 24, 377–391. DOI: 10.1016/j.gr.2012.10.006

Özkaymak, Ç., Yıldız, A., Karabaşoğlu, A.. 2017. Determination of geotourism potential. Geological Bulletin of Turkey, 60, 259–282.

Prelević, D., Akal, C., Foley, S. F.. 2012. Ultrapotassic mafic rocks. Journal of Petrology, 53, 1019–1055. DOI: 10.1093/petrology/egs008

Sims, P. A., Mann, D. G., Medlin, L. K. 2006. Evolution of the diatoms. Phycologia, 45, 361–402. DOI: 10.2216/05-22.1

Stockton, C. M., Fritsch, E. 1987. Infrared spectroscopy in gem identification. Gems & Gemology, 23, 18–26.

Taylor, D. G., Nenadic, C. M., Crable, J. V. 1970. Infrared spectra for mineral identification. AIHA Journal, 31, 100–108.

Uygun, A. 1976. Hırka (Kayseri) diyatomit yatağının jeokimyası. Geological Bulletin of Turkey, 19, 127–132.

Williams, L. A., Crerar, D. A. 1985. Silica diagenesis II. General mechanisms. Journal of Sedimentary Research, 55, 312–321.

Yamagishi, H., Nakashima, S., Ito, Y. 1997. High-temperature infrared spectra. Physics and Chemistry of Minerals, 24, 66–74.

Yıldırım, A., Kaya, M., Demir, H. 2021. Geochemical evolution of opaline silica. Journal of Sedimentary Petrology, 45(2), 155–172.

Yıldız, A. 1997. Seydiler (Afyon) diyatomit cevherinin jeolojisi ve izolasyon tuğlası olarak kullanılabilirliği. MSc Tezi, Afyon Kocatepe Univ., 128 s.

Yıldız, A., Kibici, Y., Emrullahoğlu, Ö. F. 1999. Seydiler (Afyon) diyatomit yatağının jeolojisi ve mineralojisi. BAKSEM'99, İzmir, 96–104.

Yıldız, A., Bağcı, M., Kibici, Y. 2003. Seydiler ve Bayat yörelerindeki yarı kıymetli süstaşlarının jeolojisi. I. Gemoloji Sempozyumu, Ankara, 60–75.

Yıldız, A., Gürel, A., Dursun, Y. G. 2017. Diatom community and palaeoenvironmental properties. Journal of African Earth Sciences, 134, 276–291. DOI: 10.1016/j.jafrearsci.2017.06.024